Advanced Powder Technology 32 (2021) 2591–2604

Contents lists available at ScienceDirect

Advanced Powder Technology

journal homepage: www.elsevier.com/locate/apt

Original Research Paper

Impact of hydrophilic binders on stability of lipid-based sustained release matrices of quetiapine fumarate by the continuous twin screw melt granulation technique

Dinesh Nyavanandi [a], Venkata Raman Kallakunta [a], Sandeep Sarabu [a], Arun Butreddy [a], Sagar Narala [a], Suresh Bandari [a], Michael A. Repka [a,b,*]

[a] Department of Pharmaceutics and Drug Delivery, School of Pharmacy, The University of Mississippi University, MS 38677, USA
[b] Pii Center for Pharmaceutical Technology, The University of Mississippi, University, MS 38677, USA

ARTICLE INFO

Article history:
Received 18 January 2021
Received in revised form 11 May 2021
Accepted 21 May 2021
Available online 30 May 2021

Keywords:
Sustained release
Twin screw melt granulation
Dose dumping
Phase separation, stability

ABSTRACT

Dose dumping is the major drawback of sustained release (SR) matrices. The current research aimed to develop the stable lipid-based SR matrices of quetiapine fumarate (QTF) using Geleol™ (glyceryl monostearate; GMS) as the lipid matrix carrier and Klucel™ EF (HPC EF), Kollidon® VA64, and Kollidon® 12PF as hydrophilic binders. Formulations were developed using advanced twin screw melt granulation (TSMG) approach and the direct compression (DC) technique. Compared with the blends of DC, the granules of TSMG exhibited improved flow properties and tabletability. Solid-state characterization by differential scanning calorimetry of the prepared granules exhibited the crystalline nature of the lipid. Fourier transform infrared spectroscopy demonstrated no interaction between the formulation ingredients. The compressed matrices of TSMG and DC resulted in the sustained release of a drug over 16–24 h. Upon storage under accelerated conditions for 6 months, the matrices of TSMG retained their sustained release characteristics with no dose dumping in alcohol, whereas the matrices of DC resulted in the dose dumping of the drug attributing to the loss of matrix integrity and phase separation of lipid. Thus, it is concluded that the uniform distribution of a softened binder into a molten lipid carrier results in the stable matrices of TSMG.

1. Introduction

Oral medication is a popular route for drug delivery due to its ease of administration, lack of pain, affordable cost, and lack of required assistance of health care providers during administration [1,2]. The oral dosage form occupies a significant share of the pharmaceutical sector. It can be inferred that 50–60% of the products being approved annually belong to the category of oral dosage forms (tablets/capsules/granules/powders). Of these, a significant portion (98%) refers to immediate-release dosage forms [3]. A very minute portion is occupied by sustained release products due to their complex manufacturing process and colossal investment [4]. Due to a drug's short half-life ($t_{1/2}$), in order to maintain a prolonged plasma drug concentration, patients prescribed with immediate-release dosage forms need frequent administration of the medications, which is a challenging task for patients with pre-existing conditions, such as Alzheimer's disease [4,5]. This issue shows the need for developing SR formulations that can sustain drug release for a prolonged period of time and reduce the frequency of dosing.

The tablets of SR formulations that are being developed must satisfy specific physical requirements such as hardness, content uniformity, and friability. To achieve these characteristics, formulators will employ suitable manufacturing processes, such as direct compression (DC), wet granulation, dry granulation, and recent melt granulation. However, each of these manufacturing techniques has advantages and disadvantages. DC involves the mixing of active pharmaceutical ingredients (APIs) with excipients (binders and diluents), followed by compression with no additional processing steps. However, this technique is not suitable for blends with poor flow and poor compressibility. Granulation techniques enhance the flow properties and compressibility of the formulation

* Corresponding author at: Distinguished Professor and Chair, Department of Pharmaceutics and Drug Delivery, School of Pharmacy, The University of Mississippi, University, MS 38677, USA.
E-mail address: marepka@olemiss.edu (M.A. Repka).

https://doi.org/10.1016/j.apt.2021.05.040
0921-8831/

blend and maintain a uniform distribution of ingredients with tablet integrity. However, wet granulation is not suitable for moisture-sensitive drugs, and blends processed by dry granulation will result in low tablet hardness. The advancement of the melt granulation technique has resolved some of the associated disadvantages of the above conventional techniques. With this approach, granulation is aided by a molten granulating agent without using liquids or solvents, making the process solvent-free green technology and suitable for moisture-sensitive drugs. The molten material is distributed uniformly between the particles, thereby forming agglomerates with improved flow, compressibility and content uniformity, resulting in a quality formulation [6]. This approach makes the technique unique among the granulation strategies for developing SR formulations. In recent years hot melt extrusion (HME) with wide variety of applications is being employed for continuous granulation process. Some of the applications of HME includes twin screw granulation, gastro retentive, abuse deterrent, multi component systems, and sustained release formulations [7–11].

Lipid-based excipients play an important role in enhancing bioavailability and are also being employed in developing SR and taste-masked formulations. However, the major disadvantage of the lipid-based formulations is their instability upon storage, which affects the drug release profiles. Various researchers have reported enhanced drug release profiles causing dose dumping in lipid-based matrices. Storage temperature, polymorphism, recrystallization, and phase separation were identified as the responsible factors affecting the stability of the lipid-based formulations [12–14]. An increase in the dissolution rate and stability of the lipid-based formulations upon storage has lacked in-depth investigation until now.

The main aim of the current research was to develop stable lipid-based SR matrices by the novel twin-screw melt granulation (TSMG) approach using a twin-screw extruder. Further, the role of different molecular weights and viscosity grade hydrophilic binders to maintain the SR properties of the lipid-based matrices upon storage were investigated. The rationale in selection of a twin-screw extruder was to investigate TSMG as a single step process and impart high shear, uniform mixing of materials at desired processing temperatures. Geleol™ (glyceryl monostearate; GMS), comprising 40–55% monoacylglycerols, 30–45% diacylglycerols, 5–15% triacylglycerols palmitic acid and stearic acid with an HLB value of 3, was used as a lipid carrier (melting point 54–64 °C) [15,16]. Hydrophilic polymeric excipients such as Klucel™ EF (hydroxypropyl cellulose, HPC EF; molecular weight 80,000 Daltons and viscosity 300–600 MPa.s), Kollidon® VA64 (molecular weight 45,000 Daltons and viscosity 25.2–30.8 MPa.s) and Kollidon® 12PF (molecular weight 2000–3000 Daltons and viscosity 1.3–2.3 MPa.s) were chosen as the binders based on the viscosity and molecular weight. The glass transition temperature (Tg) of the binders was found to be 120℃, 101℃ and 90℃ for HPC EF, VA64 and 12PF, respectively. Quetiapine fumarate (QTF) with a high water solubility was used as a model drug. The rationale behind the selection of a hydrophilic drug and hydrophilic binders is to prevent the dissolution of the drug and the hydrophobicity of the binders as the rate-limiting step in achieving sustained release action of lipid based matrices. The process was carried out at a temperature greater than the melting point of the lipid carrier and above the Tg of the binders to ensure its uniform distribution between the particles in order to preserve matrix integrity throughout the shelf life. The main interest was to investigate the effect of a uniformly distributed softened binder within the lipid carrier on the stability of matrices. The optimized final formulations of the TSMG process were also processed by direct compression (DC) and evaluated as reference samples.

2. Materials and methods

2.1. Materials

Quetiapine fumarate was a kind gift from RIA International LLC (NJ, USA), and the lipid carrier Geleol™ (glyceryl monostearate; GMS) was a gift from Gattefosse (NJ, USA). The hydrophilic binders, namely, Klucel™ EF (HPC EF) with particle size distribution (d_{90}) 150–250 μm, Kollidon® VA64 (VA64) and Kollidon® 12PF (12PF) with particle size distribution of (d_{90}) 50–250 μm, were supplied by Ashland (DE, USA) and BASF (USA) respectively. Avicel PH® 102 (Microcrystalline Cellulose; MCC102) was donated by FMC Biopolymer (USA), and magnesium stearate was purchased from Alfa Aesar (USA).

2.2. Preparation of the physical mixtures

All the raw materials, i.e., the lipid, binders, and diluent along with the active pharmaceutical ingredient (API), were weighed in required quantities and co-sifted through a # 30 ASTM mesh. The sifted materials were blended for 10 min at 20 RPM in a V-cone blender (Maxiblend®, Globe Pharma, NJ, USA) and processed for twin screw melt granulation (F1 to F16). Similarly, the blends of the direct compression formulations (F17 to F20) were prepared by sifting all the formulation ingredients excluding the lubricant through a #30 ASTM mesh, followed by the blending (pre-lubrication) of materials for 10 min at 20 RPM and the lubrication for 3 min at 20 RPM. The batch formula for all the trials conducted is presented in Table 1. All the blends were prepared with quantities of 100.0 g (initial trials) and 200.0 g (final optimized formulations). Prior to dispensing the formulation ingredients, the pellets of GMS (lipid) were milled in a standard coffee blender and sifted through a #30 ASTM mesh.

2.3. Twin screw melt granulation

Melt granulation was performed using an 11 mm twin screw extruder (Process 11 Thermo Fischer Scientific). All the granulations were processed without using a die at the discharge point. The process temperature was maintained at 10 – 30℃ above the glass transition temperature (Tg) of the binders for softening and uniform distribution. The temperatures of zone-2 and the die were maintained at ambient conditions (25 ℃), and the temperatures of zone-3 to zone-8 were maintained at 130℃ for the HPC EF and VA64 formulations and 100℃ for the 12PF formulations. The feed rate of 2.5 g/min and screw speed of 50 RPM were maintained constant for all granulations. An identical screw configuration was employed for all the formulations with two mixing zones, one with seven kneading elements with a 60° offset angle (zone-5) and the other with five kneading elements with a 30° offset angle (zone-8). The detailed screw configuration is captured in Fig. 1(a). The flow rate of the physical mixture was calibrated before batch initiation to ensure uniform flow of the material into the barrel throughout the process time. The equipment was allowed to equilibrate for 10 min before feeding the material into the barrel. Granules collected during the initial 5 min were discarded to achieve uniform torque and blend occupancy within the barrel. The collected granules were allowed to cool to room temperature and sifted through the #20 ASTM mesh. The sifted granules were lubricated using magnesium stearate (0.3%), which was pre-sifted through the #40 ASTM mesh and blended for 3 min at 20 RPM.

2.4. Flow properties

The physical mixtures and final blends of the TSMG and DC formulations were evaluated for angle of repose and Carr's index using the equations described below [17].

Table 1
Compositions of various formulations of twin screw melt granulation (F1-F16) and direct compression (F17-F20).

INGREDIENTS[a]	F1	F2	F3	F4	F5	F6	F7	F8	F9	F10	F11	F12	F13	F14	F15	F16	F17	F18	F19	F20
QTF	34.60	34.60	34.60	34.60	34.60	34.60	34.60	34.60	34.60	34.60	34.60	34.60	28.83	28.83	28.83	31.45	28.83	28.83	28.83	31.45
GMS	15.00	15.00	15.00	7.50	7.50	7.50	10.00	10.00	10.00	12.50	12.50	12.50	10.00	12.50	20.00	20.00	10.00	12.50	20.00	20.00
Klucel™ EF	5.00	–	–	5.00	–	–	5.00	–	–	5.00	–	–	5.00	–	–	–	5.00	–	–	–
Kollidon® VA64	–	5.00	–	–	5.00	–	–	5.00	–	–	5.00	–	–	5.00	–	–	–	5.00	–	–
Kollidon® 12PF	–	–	5.00	–	–	5.00	–	–	5.00	–	–	5.00	–	–	5.00	5.00	–	–	5.00	5.00
Avicel 102	45.10	45.10	45.10	52.60	52.60	52.60	50.10	50.10	50.10	47.60	47.60	47.60	55.87	53.37	45.87	43.25	55.87	53.37	45.87	43.25
Magnesium stearate	0.30	0.30	0.30	0.30	0.30	0.30	0.30	0.30	0.30	0.30	0.30	0.30	0.30	0.30	0.30	0.30	0.30	0.30	0.30	0.30
Matrix weight	**500.00**	**500.00**	**500.00**	**500.00**	**500.00**	**500.00**	**500.00**	**500.00**	**500.00**	**500.00**	**500.00**	**500.00**	**600.00**	**600.00**	**600.00**	**550.00**	**600.00**	**600.00**	**600.00**	**550.00**

[a] All amounts are expressed as %w/w.

$$\text{Angle of repose}: \text{Tan}(\theta) = \frac{h}{r}$$

where h = the height of the pile and
r = the radius of the pile

$$\text{Carr's index (CI)}: \text{CI} = \frac{\text{TD} - \text{BD}}{\text{TD}}$$

where BD and TD are the bulk density and tapped density, respectively.

2.5. Particle size distribution (PSD)

The PSD was monitored for the granules of the TSMG process using a vibratory sieve shaker (Performer III SS-3, Gilson Inc., Ohio, USA) at an amplitude of 5 for 5 min and 60 taps/min. A weighed quantity of the blend (10.0 g) was added to the vibratory shaker and allowed for blend separation depending on particle size using #20, #30, #40, #60, #120 and #200 ASTM sieves. The retained contents of each sieve were collected, weighed, and calculated for its % contents.

2.6. Fabrication of the SR matrices

The lubricated blends of the TSMG and DC formulations were compressed using a rotary tablet press (Piccola, Argentina) with 10 mm round concave punches with a target hardness of 10–12 kp at 20 rpm speed. The main compression force was recorded using "The Director" software (version 4.00.05). Compressed matrices were collected at regular intervals of 3 min during compression and evaluated for hardness (VK200, Optimal Control). Each compressed matrix contained 173.0 mg of quetiapine fumarate, which is equivalent to 150.0 mg of quetiapine.

2.7. Evaluation of the SR matrices

The compressed matrices were evaluated for weight variation, hardness, and friability. Ten matrices of each batch were weighed individually, and the mean and SD were calculated. The mechanical strength of the matrices was tested using a hardness tester. The friability was determined by taking the weight equivalent of the matrices to 6.5 g and loading the matrices into the drum and operated for 4 min at 25 revolutions/min (Vanderkamp® 10801, Vankel Industries, Inc. USA). The collected matrices were dedusted, weighed and calculated for % weight loss using the following equation:

$$\%\text{Friability} = \frac{\text{Initial weight} - \text{Final weight}}{\text{Initial weight}} \times 100$$

2.8. Content uniformity

Five matrices of each batch were crushed to a fine powder, and a weight equivalent to 100 mg of the drug was weighed and transferred into a volumetric flask. The volume consisted of acetonitrile and water (1:1 ratio) [as per USP]. The sample was sonicated for 30 min, and an aliquot of 1.5 ml was transferred into an Eppendorf tube with a 0.22 μm filter and centrifuged at 10000 rpm for 10 min (AccuSpin Micro 17, Fisher Scientific, Germany). The supernatant was collected, suitably diluted and analyzed for drug concentration using a UV–visible spectrophotometer (Genesys 180, WI, USA) at 246 nm. All evaluations were performed in triplicate, and the mean ± SD of the results was reported. Similarly, the content uniformity of the granules (TSMG) and the pre-lubricated blend of the direct compression formulations were evaluated by taking 5.0 g of the blend quantity.

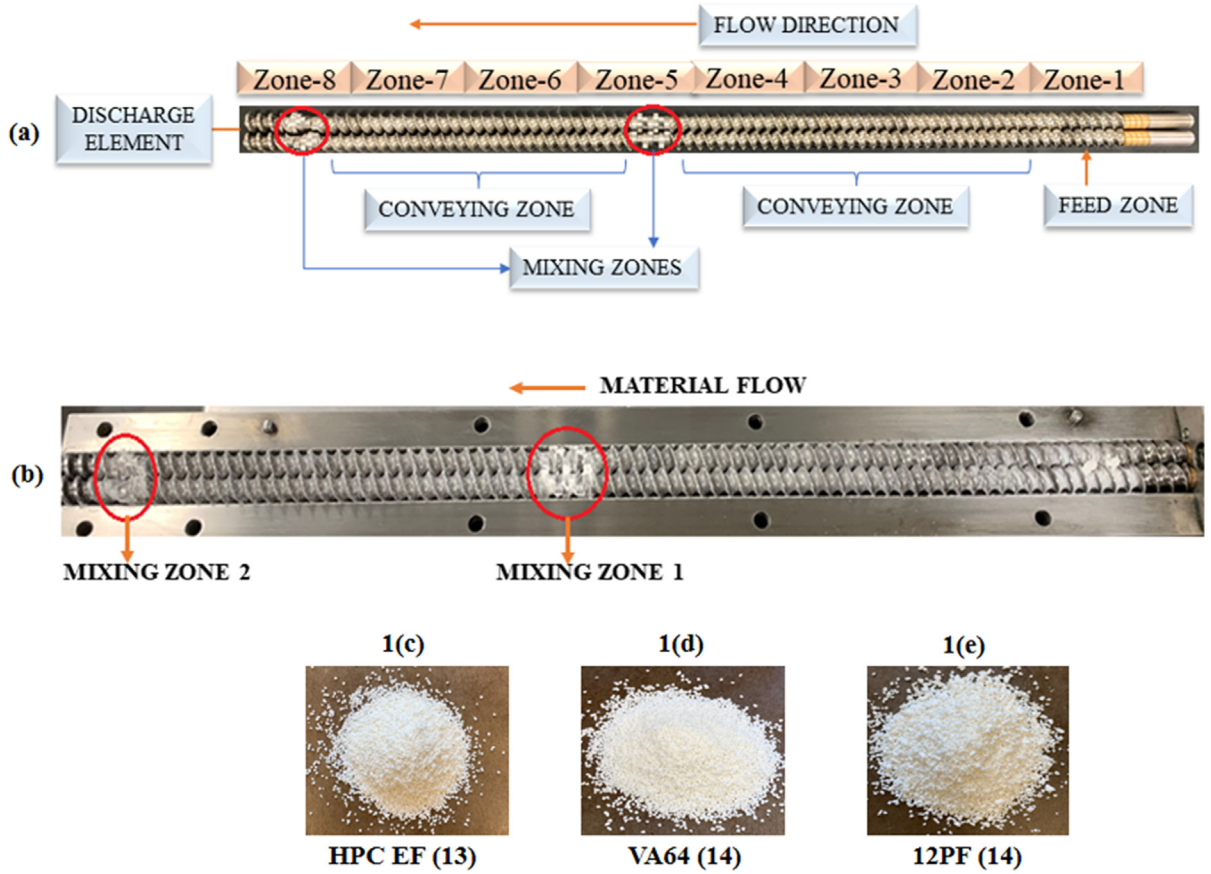

Fig. 1. (a) Detailed screw configuration employed in TSMG; Fig. 1(b) Inner view of the barrel zones following post granulation; and Fig. 1(c) (d) (e) granules of the HPC EF; VA64; and 12PF formulations.

2.9. Morphology of the melt granules

The surface morphology of the melt granules was evaluated using scanning electron microscopy (SEM, JSM-7200FLV, JOEL, Peabody, MA, USA) with a voltage of 5 kV. All the samples were adhered to the SEM stubs using double adhesive tape. Prior to imaging, all the samples were coated with platinum under an argon atmosphere using a Denton Desk V TSC sputter coater (Denton Vacuum, Moorestown, NJ, USA).

2.10. Differential scanning calorimetry (DSC)

The pure GMS, physical mixtures (PM), granules and matrices of TSMG were investigated to observe any shift in the melting peak of the lipid (GMS). The samples were analyzed using a Discovery DSC 25 (TA Instruments DSC, New Castle, DE, USA) mounted with an RCS90 cooling device. The temperature and heat capacity of the instrument were calibrated using indium and sapphire standards. A sample quantity of 5 mg was accurately weighed in a Tzero aluminum pan and sealed using Tzero lids. The samples were equilibrated at 25 °C for 1 min, followed by heating at a rate of 10 °C/min up to 200 °C while maintaining an inert atmosphere using nitrogen gas at a flow rate of 50 ml/min.

2.11. Fourier transform infrared spectroscopy (FTIR)

The drug-excipient interactions and characteristic peaks of the lipid were monitored using an Agilent Cary 660 FTIR spectrometer (Agilent Technologies, Santa Clara, CA, USA). The sample was prepared by adding a trace amount on top of the diamond crystal, followed by compression using a MIRacle high-pressure clamp. The sample was scanned 16 times from 600 to 4000 cm^{-1} with a resolution of 4 cm^{-1}. The instrument was mounted with ATR (Pike Technologies, Madison, WI, USA) fitted with a single bounce, diamond-coated ZnSe internal reflection element.

2.12. In vitro drug release studies

The matrices of TSMG and DC formulations were evaluated for drug (quetiapine) release profiles. A dissolution test (USP, Test-4) was performed in water (900 ml) using a USP type II apparatus (SR8-plus™, Hanson Research) at a 100 rpm paddle speed and at a 37 ± 0.5℃ bath temperature. At each time point (0.5, 1, 2, 4, 6, 8, 12, 16, 20 and 24 h), 1 ml of sample was collected and filtered through 10 μm dissolution filters. The samples were diluted suitably, and the absorbance was recorded using a UV–visible spectrophotometer at 246 nm.

2.13. Drug release kinetics

The in vitro drug release kinetics of all the optimized formulations of TSMG and DC were interpreted using the following various mathematical models [18–22].

$$\text{Zero} - \text{orderkinetics} : C_t = C_0 + K_0 t$$

where C_t = the amount of drug release at time t
C_0 = the amount of drug released at time 0
K_0 = zero-order rate constant

$$\text{First}-\text{orderkinetics}:\log C=\log C_0-\frac{Kt}{2.303}$$

where K = first-order rate constant
C_0 = the initial concentration of drug
C = the percentage of drug remaining at time t.

$$\text{Higuchimodel}:Q=K_H t^{1/2}$$

where Q = the amount of drug release at time t
K_H = Higuchi dissolution constant

$$\text{Korsmeyer}-\text{Peppasmodel}:\log\frac{Mt}{M\infty}=\log K_{kp}+n\log t$$

where Mt = the amount of drug released in time t,
$M\infty$ = the amount of drug released after time ∞,
n = diffusional exponent
K_{kp} = Korsmeyer-Peppas release constant

$$\text{Hixson}-\text{Crowellmodel}:W_0^{\frac{1}{3}}-W_t^{\frac{1}{3}}=K_{HC}t$$

where W_0 = the initial amount of drug in dosage form
W_t = remaining amount of drug in dosage form at time t
K_{HC} = Hixson-Crowell constant

2.14. Matrix erosion index (EI)

The erosion index of the matrices was evaluated by slightly modifying the procedure described by Wang, L et al. [23]. The initial weight (W1) of the matrices was recorded, and then the matrices were dropped into a dissolution vessel (900 ml; water) operated at a paddle speed of 100 rpm and a temperature of 37 ± 0.5 °C. At similar dissolution time points, the matrices were collected by discarding the dissolution media without affecting their integrity. The weight (W2) of the matrices was recorded after allowing them to dry at 50 °C for 24 h (Econtherm laboratory oven, Virginia, USA). The percentage erosion index (%EI) was calculated using the equation:

$$\%EI=\frac{W1-W2}{W1}\times 100$$

2.15. Distribution of the lipid

The distribution of the lipid within the matrices of TSMG and DC formulations was studied. Powdered GMS was coated with a lipid soluble dye (Nile red) by triturating a mixture of the lipid and dye (0.5 mg) in a mortar and pestle. The obtained dye-coated lipid was utilized in developing formulations of TSMG and DC. The compressed matrices were stored at 40 ± 2℃/75 ± 5% RH for three months, and the distribution of the lipid was monitored upon storage; the later observations were compared with initial observations (0 days).

2.16. Stability studies

The selected formulations of TSMG and DC were loaded for stability under accelerated conditions (40 ± 2℃/75 ± 5% RH) for six months in a laboratory stability chamber (Caron 6030). Forty matrices of each batch were packed in an HDPE containers (20 s count) with silica gel sachets (2 g/bottle). The samples were removed from the container at respective time points (1, 2, 3 and 6 months) and analyzed for hardness, drug content, in vitro drug release, DSC and dose dumping studies. The in vitro drug release profiles of the stability samples were compared with the initial results (0 days) by calculating the similarity (f2) and dissimilarity factors (f1). The similarity and dissimilarity factors were calculated using the following equations [24,25]:

$$f_2=50\log\{\left[1+\left(\frac{1}{n}\right)\sum_{t=1}^{n}(R_t-T_t)^2\right]^{-\frac{1}{2}}x100\}$$

$$f_1=\{[\sum_{t=1}^{n}|R_t-T_t|]/[\sum_{t=1}^{n}R_t]\}x100$$

where n is the number of time points, R_t is the cumulative drug release rate of the reference sample, and T_t is the cumulative drug release rate of the test sample at predetermined time points. A similarity factor ≥ 50 indicates the closeness between the values of the test and reference samples. Whereas a value (f1) close to 0 indicates less dissimilarity between the samples. Based on the stability data, the optimized stable formulations were studied for dose dumping.

2.17. Alcohol-induced dose dumping (AIDD)

An AIDD study for the stable formulations of TSMG was conducted employing water,40% ethanol in water, 0.1 N HCl and 40% ethanolic 0.1 N HCl as the dissolution media [26]. The initial (0 days) dose dumping data of the stable TSMG formulations were generated at the time of study by compressing a fresh sample of matrices. The release profiles of freshly compressed matrices were verified by conducting in vitro dissolution studies, as described in section 2.12. All the dissolution parameters were maintained to be similar to those of the in vitro drug release study (Section 2.12). The samples were collected every 15 min for 2 h. Collected samples were analyzed using a UV–visible spectrophotometer at 246 nm using dissolution media as a blank.

3. Results and discussion

3.1. Twin screw melt granulation

All melt granulation experiments (F1-F16) were performed successfully by melting the lipid carrier and softening binder and maintaining the remainder of the formulation ingredients (API and diluent) in a non-molten state (i.e., dry state). The molten and softened materials among the formulation ingredients aided in particle agglomeration, and upon cooling, the materials hardened, resulting in granule formation [27]. The residence time was found to be 1.5 min, exposing the formulation ingredients to thermal energy for a noticeably short time and preserving the stability of lipid. The formation of granules and the level of torque were recorded for all melt granulation experiments. Granule formation was observed even at low binder (5%) and lipid (7.5%) concentrations [28]. The physical texture of the granules that were verified manually revealed harder granules for formulations with high molecular weight binders, which is in line with the results reported by Jinjiang Li et al. [29]. Improved granulation efficiency was observed with increasing binder viscosity and increasing lipid concentration [27,30]. Increasing the lipid concentration resulted in an increased concentration of molten material available for agglomeration and granule formation. The viscosity of polymeric binders decreases with increasing temperature. However, all three binders under investigation have demonstrated a decreasing order of melt viscosity at their respective processing temperatures. The following trend was reported at the investigated processing temperatures for three different binders (HPC EF > VA64 > 12PF). This is correlated with the high molecular weight and viscosity of binders in solution [31,32]. All the barrel zones were found to be clean with no sticking of the material to the screw elements, thus preventing the in-process material loss of the active ingredient. The lubrication effect of molten lipid might have prevented the sticking of the formulation ingredients to the barrel surface. The inner view of barrel zones soon after completion of granulation is shown in

Table 2
Process parameters of twin screw melt granulation.

Batch#	Binder	Lipid (%)	Granule formation	Screw speed (RPM)	Feed rate (g/min)	Torque (%)
F1	HPC EF	15.0	Yes	50	2.47 ± 0.05	7.0–9.0
F2	VA64	15.0	Yes	50	2.52 ± 0.05	7.0–8.0
F3	12PF	15.0	Yes	50	2.47 ± 0.06	6.0–8.0
F4	HPC EF	7.5	Yes	50	2.48 ± 0.06	5.0–7.0
F5	VA64	7.5	Yes	50	2.51 ± 0.05	4.0–6.0
F6	12PF	7.5	Yes	50	2.49 ± 0.07	2.0–3.0
F7	HPC EF	10.0	Yes	50	2.49 ± 0.04	6.0–7.0
F8	VA64	10.0	Yes	50	2.51 ± 0.06	5.0–7.0
F9	12PF	10.0	Yes	50	2.46 ± 0.03	3.0–4.0
F10	HPC EF	12.5	Yes	50	2.51 ± 0.05	7.0–8.0
F11	VA64	12.5	Yes	50	2.53 ± 0.05	6.0–8.0
F12	12PF	12.5	Yes	50	2.50 ± 0.04	4.0–6.0
F13	HPC EF	10.0	Yes	50	2.49 ± 0.04	6.0–7.0
F14	VA64	12.5	Yes	50	2.51 ± 0.03	6.0–8.0
F15	12PF	20.0	Yes	50	2.50 ± 0.02	8.0–10.0
F16	12PF	20.0	Yes	50	2.49 ± 0.04	8.0–10.0

Fig. 1(b). Overall, the low torque values (6–10%) can be attributed to the uniform distribution of the molten lipid throughout the inner barrel surface and could also be attributed to the low melt viscosity and lubrication effect of the lipid [33,34]. The yield reconciliation for all the studied batches was found to be 97.0 – 98.0%, which shows the efficiency of the manufacturing technique in preventing the process loss of the material. The process parameters were recorded in Table 2.

3.2. Pre-compressional characteristics of the blend

The physical mixtures, granules of TSMG and pre-lubricated blends of the DC formulations were evaluated for their flow properties, and the obtained results are presented in Supplementary Table 1. The poor flow of the blend and the non-homogeneous distribution of active ingredients affect the quality of drug products, leading to product failure [35]. The final blends of TSMG and DC exhibited better flow characteristics than the respective physical mixtures. The formulations of TSMG exhibit superior flow characteristics over the lubricated blends of DC, thus proving the efficiency of the melt granulation technique for improving the flow properties. The angle of repose and Carr's index of the TSMG formulations were found to be between 25.80 and 28.33°and 11.45–13.54, respectively, indicating excellent to good flow when compared with the lubricated blend of direct compression. The content uniformity of the active was preserved, where the assay of TSMG and DC formulations was found to be between 98.01 and 101.45%.

3.3. Particle size distribution

The particle size distribution plays an important role in determining the product performance, such as the flow properties, dissolution, matrix strength, friability, and content uniformity. The particle size distribution of the TSMG formulations (F1-F16) is recorded in Fig. 2. All the formulations resulted in granules of size < 841 μm. Approximately 56–68%, 48–60% and 33–50% of

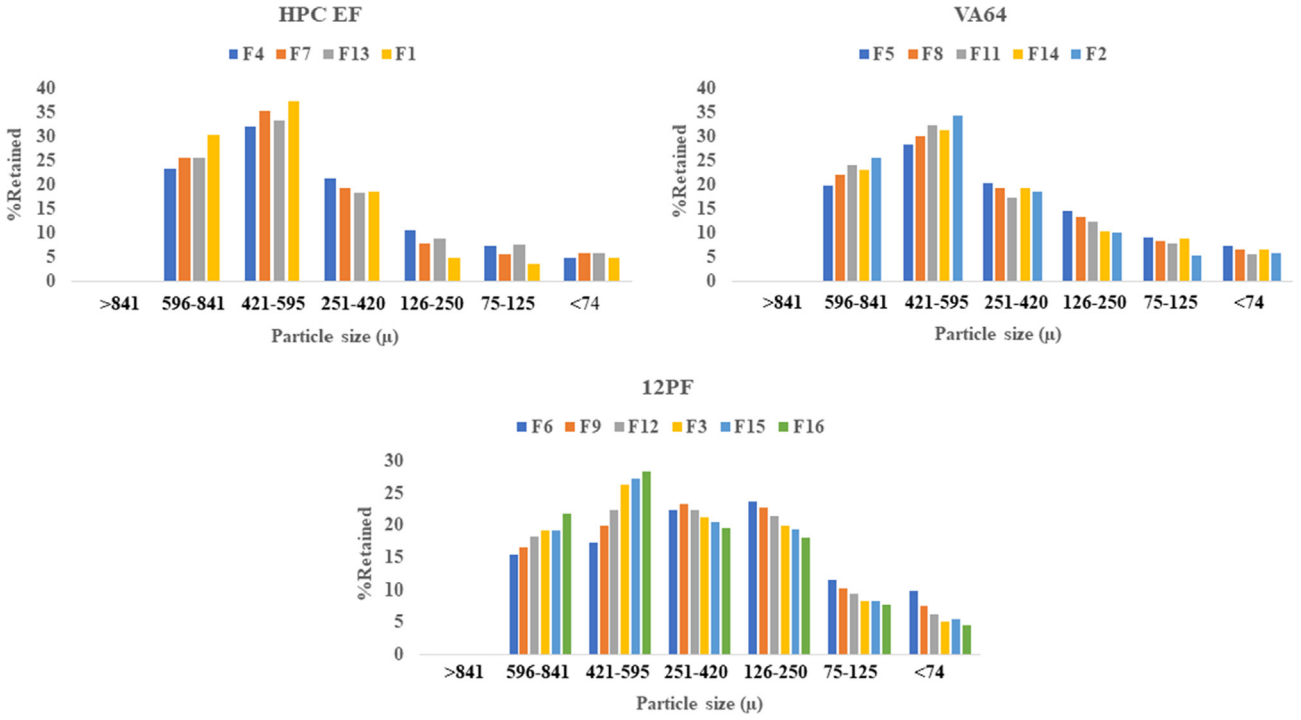

Fig. 2. The particle size distribution of the TSMG formulations using HPC EF, VA64, & 12PF binders.

the granules were found to be between 595 and 841 μm for the HPC EF, VA64 and 12PF formulations, which are in line with the viscosity of the binders. The higher the viscosity is, the greater the number of large granules. Similarly, the portion of fines (<125 μm) was found to be increased (8–13%, 11–17% and 12–21%) with decreasing order of the binder viscosity and molecular weight. It can be inferred that the lower the viscosity is, the lower the binding property of the binders. It was observed that the number of granules formed was influenced by various formulation variables, such as the viscosity and molecular weight of the binders and the concentration of molten lipid [29]. The increased viscosity and concentration of the molten material resulted in enhanced cross-linking of particles with improved efficiency [36,37]. From Fig. 2, it can be observed that a major portion of the granulated blend existed at approximately 421–841 μm for formulations of HPC EF and VA64, whereas a widespread particle distribution (250–841 μm) was observed for 12PF formulations. The wide distribution of granules for 12PF formulations can be attributed to its lower viscosity and poor binding property. Following twin screw melt granulation, all the collected granules were soft enough to pass through a #20 ASTM mesh. Thus, twin screw granulation is suitable for producing granules of the desired size with reduced downstream processing steps.

3.4. Evaluation of the compressed matrices

Physical parameters including the weight variation, hardness, thickness, friability, and content uniformity of all the compressed matrices of TSMG (F1-F16) and DC (F17-F20) studies are shown in Supplementary Table 2. It is clear from the obtained results that all the evaluations performed with respect to the weight variation, hardness and thickness are within acceptable limits. The weight of the matrices was within ± 1% of the target weight, and the hardness was within the acceptable limits of 10–12 kp. The friability of the matrices was < 1%, which shows the rigidity of the matrix to withstand external stress experienced during packing, storage, and transportation. The low matrix friability of TSMG formulations when compared with matrices of DC can be attributed to the uniform distribution of a softened binder as a result of shear and its efficient bonding with the remainder of the formulation ingredients in extruder barrel. The compression force required to attain the target hardness (10–12 kp) was determined to be dependent on the molecular weight of the binder, with increasing molecular weight (12PF < VA64 < HPC EF) of the binder, the compressional force required to compress the matrix was increased [29]. The compression force needed to fabricate the matrices of TSMG (F1-F16) comprising HPC EF, VA64, and 12PF binders was approximately 884.6–887.2, 816.3–820.7 and 755.5–760.6 kPa, respectively. A similar trend of the compression force was observed for the DC formulations (F17-F20), and the compression force required was higher than that of the melt granulation formulations due to poor compressibility and the non-uniform distribution of the formulation ingredients. The compression forces required for the DC blends comprising HPC EF, VA64 and 12PF binders were 910–914.6, 850.4–854.2 and 800.1–803.2 kPa, respectively. Content uniformity was between 98.32 and 101.32%, which is in line with that of the blend assay results indicating a uniform distribution of API throughout the manufacturing process.

3.5. Surface morphology

The surface morphology of the granules of TSMG and its corresponding physical mixtures were studied and captured in Fig. 3. The pure API (Fig. 3A) and physical mixtures (top right corner of respective image) depict the irregular morphology and irregular symmetry of the particles. The surface morphology of the melt granules for the formulations of HPC EF (Fig. 3B), VA64 (Fig. 3C), and 12PF (Fig. 3D) shows the agglomeration of incorporated formulation ingredients with the aid of a molten lipid carrier and softened binder, resulting in an uneven surface morphology. The melt granulation of active material in the presence of a molten lipid (binary mixture) would have resulted in a smooth surface morphology [38], and the rough or uneven surface morphology of the obtained granules of TSMG can be attributed to incorporation of all the tableting ingredients within the granulation process. The symmetry of the granules was closely spherical, which can be attributed to improved flow and is in accordance with the flow properties of the granules. Thus, TSMG played an important role in the agglomeration of the formulation ingredients, thereby promoting the flow and compressibility of the physical mixtures.

3.6. Differential scanning calorimetry

Thermal scans were performed for the pure API, lipid carrier (GMS), physical mixture (PM), granules (TSMG), and finished product (matrices of TSMG) to monitor the nature of the lipid and drug throughout the process. The thermal scan of QTF demonstrated an endothermic peak at 176℃ indicating crystalline nature of QTF. All the scans performed revealed the existence of the drug and lipid in the crystalline form within the formulations (Fig. 4). The single melting peak of lipid suggests its existence in stable (β) form. Similarly, the endothermic peak of QTF at 176℃ within the physical mixtures, granules, and matrices indicates existence of QTF in crystalline form throughout the melt granulation process. The short residence time (1.5 min) of the material within the extruder barrel might have not affected the stability of the lipid when exposed to a higher temperature (130℃). No shift in the melting peak of the lipid was observed, indicating no interactions with other formulation ingredients and preserving its stability [39].

3.7. Drug excipient compatibility (FTIR)

FTIR analysis was performed for the drug (QTF), lipid carrier (GMS), physical mixture, granules, and matrices of the TSMG and DC formulations. All the scans that were conducted are exhibited in Fig. 5. QTF showed characteristic peaks at 649.9 and 659.5 cm^{-1} representing C-S-C stretching and at 1332.56 cm^{-1} representing C-N stretching. The peaks at 1409.7, 1060.6 and 1596.7 were identified as aliphatic H-bending, -C-O-C symmetrical stretching and carbonyl stretching of fumarate, respectively [40]. Similarly, the lipid carrier has characteristic peaks at 2913.9, 2952.46, 2848.3 cm^{-1}, indicating $-CH_2$ stretching vibrations, and the peaks at 1729.82 and 1200–1000 cm^{-1} represent carbonyl stretching peaks (C═O) and stretching peaks of C-H [41–43]. No change in the IR absorption bands was observed within the formulations, indicating drug and lipid identity without undergoing any chemical interactions with other formulation ingredients and the existence of the lipid in its original form without undergoing any polymorphic changes and degradation.

3.8. In vitro drug release

The drug release profiles of the TSMG formulations (F1-F16) are represented in Fig. 6. Drug release was optimized by altering the lipid and diluent concentrations. Increasing the lipid concentration retarded the drug release due to its poor water solubility. At a 15% (F1-F3) lipid concentration, complete drug release was not observed for any of the three binder formulations. However, the matrices of HPC EF (F1) resulted in a 27% drug release, and the matrices of VA64 (F2), 12PF (F3) resulted in a 34% and 67% drug release at the end of 24 h. These results were found to be in line with the order of the binder viscosity and molecular weight (HPC

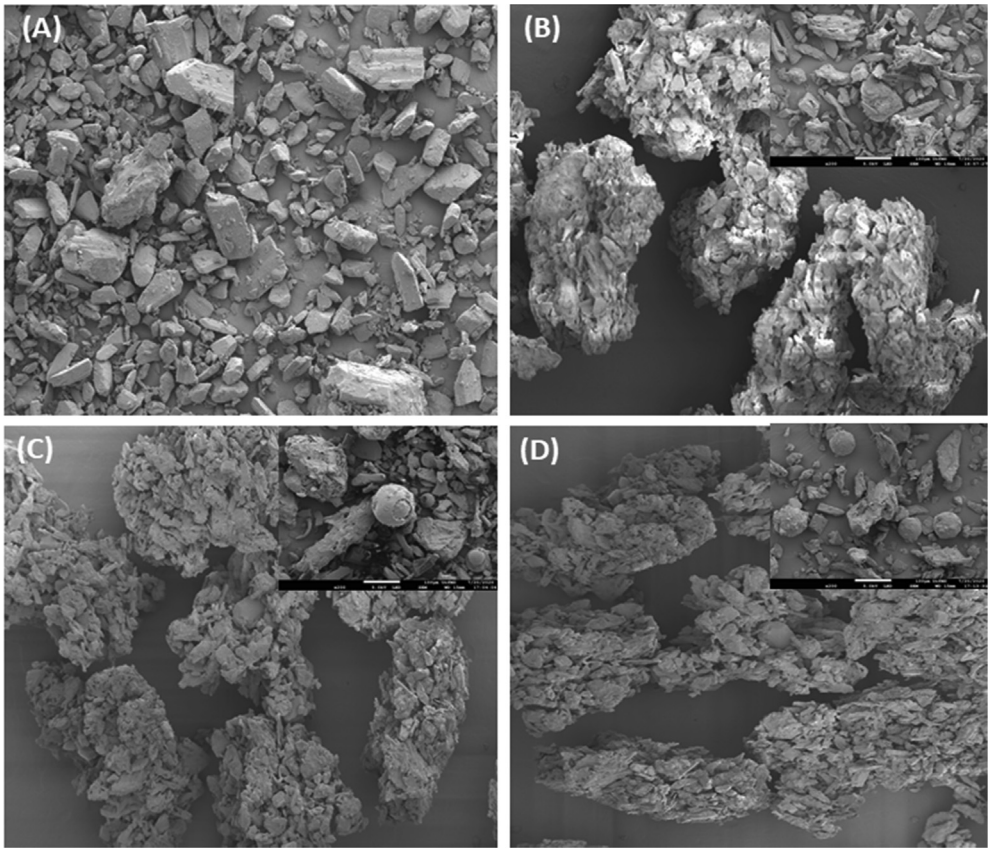

Fig. 3. Surface morphology of (A) pure API; (B) physical mixture and granules of HPC EF F13; (C) VA64 and F14; and (D) 12PF and F16.

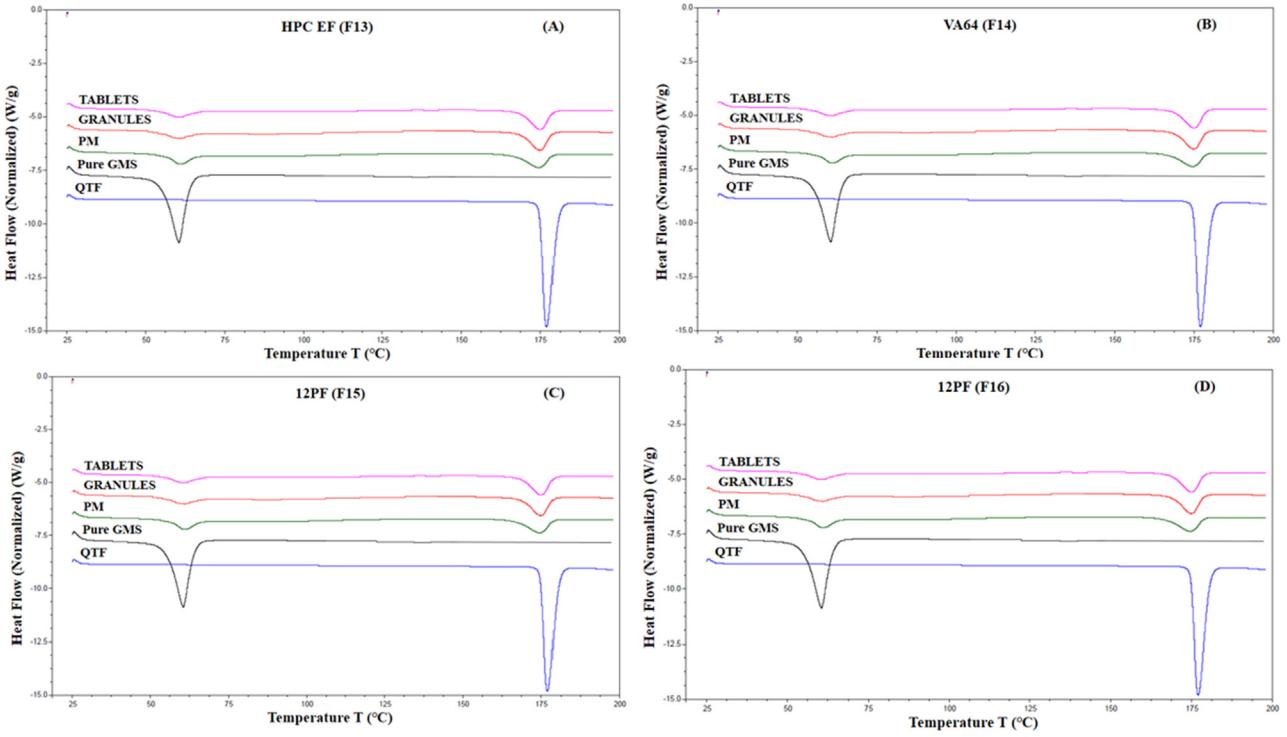

Fig. 4. Heat flow scans of the optimized TSMG formulations: (A) HPC EF, (B) VA64, and (C) & (D) 12PF formulations.

EF > VA64 > 12PF). The formulations of low-viscosity binders resulted in faster drug release due to the faster dispersibility of the matrix. A further reduction in the lipid concentration to 7.5% (F4-F6) resulted in dose dumping of the drug, where complete drug release (>90%) was attained in 4–6 h for all three binder formulations. At a 10% lipid concentration, >90% drug release was obtained

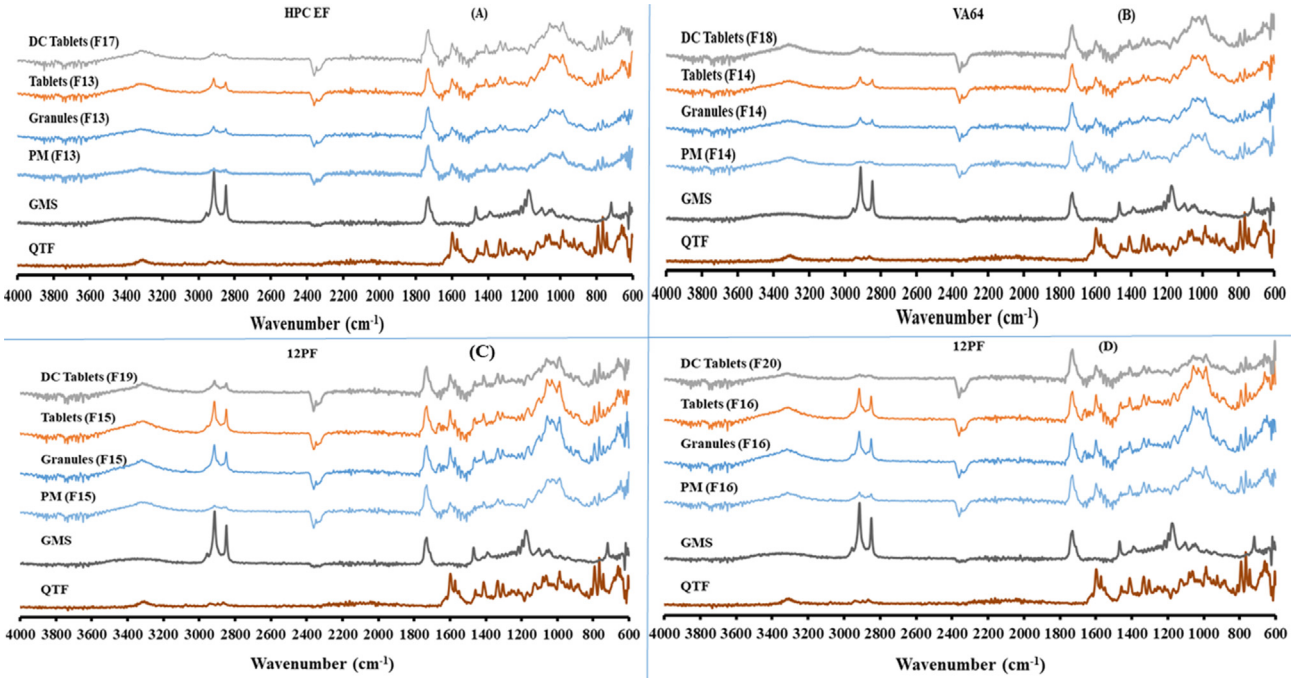

Fig. 5. FTIR spectra of (A) HPC EF formulations, (B) VA64 formulations, and (C) and (D) 12PF formulations.

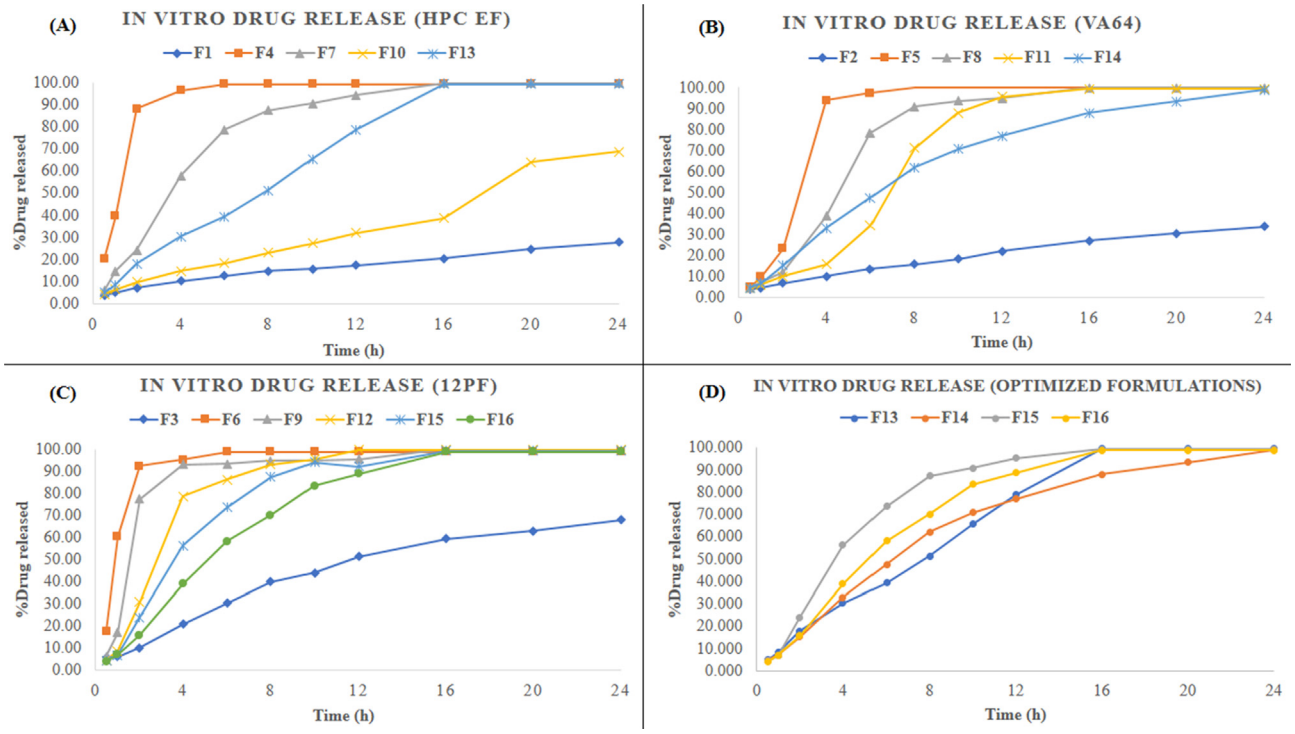

Fig. 6. In vitro drug release profiles of TSMG: (A) formulations of HPC EF (B) formulations of VA64 (C) formulations of 12PF and (D) optimized formulations of TSMG HPC EF (F13), VA64 (F14), 12PF (F15 & F16).

in 10 h for the HPC EF (F7) and VA64 (F8) formulations, and a > 90% drug release was obtained for 12PF (F9) in 4 h. The formulation of HPC EF (F10) with a 12.5% lipid concentration resulted in incomplete drug release (69%) at the end of 24 h, whereas an improved release profile (slow drug release) was observed during the initial hours of dissolution, followed by fast drug release for the VA64 (F11) formulation. At this lipid concentration (12.5%), no sustained release action was observed for matrices of 12PF (F12). The matrices of the 12PF formulations were found to disintegrate in the initial dissolution time points, resulting in dose dumping and fast drug release. The reason for the rapid disintegration of the 12PF matrices can be attributed to more fines resulting in increased surface area and low viscosity that leads to poor bonding when compared to the formulations of HPC EF and VA64. Chu, K. R

investigated the effect of the particle size on dissolution, where a decrease in the size of the granules (increased fines) resulted in increased dissolution, which can be attributed to an increase in the particle surface area [44].

All the above formulations of HPC EF, VA64 and 12PF with lipid concentrations ranging from 7.5% to 15% resulted in either fast drug release or incomplete release profiles. The matrices of HPC EF (F7) composed of a 10.0% lipid concentration with > 90% drug release in 10 h were controlled by reducing the drug load from 34.60% (F7) to 28.83% (F13). The matrices of HPC EF (F13) with a reduced drug load resulted in sustained drug release over a period of 16 h with a 50% drug release in 8 h and complete release in 16 h. Similarly, effect of reduced drug load was noticed for VA64 (F14) and 12PF (F15) formulations. Matrices of VA64 (F14) and 12PF (F15) with a drug load of 28.83% has resulted in sustained release of drug for 24 h and 16 h respectively. Thus, the drug load played a vital role in optimizing the release profiles. The higher the highly soluble drug concentration is, the faster the dissolution profiles, which are attributed to the greater exposure of the drug to the dissolution media [45].

However, the drug release characteristics of 12PF formulation (F15) with 87.0% of drug release in 8 h, followed by a complete release in 16 h was further investigated to study the effect of diluent concentration on drug release profiles. A reduction in diluent concentration from 45.87% (F15) to 43.25% (F16) with a decrease in tablet weight from 600 mg to 550 mg has resulted in slower drug release of 70.0% in 8 h and 100.0% in 16 h. The reduced tablet weight of F16 formulation improved the matrix integrity, which is in line with friability data and matrix erosion studies. The improved matrix integrity was facilitated by increased compactability of F16 tablets compared to F15. This may be attributed due to by increased percent of granules in F16 compared to F15. These results are in line with the data of tablet friability and matrix erosion studies.

Overall, the higher the viscosity and molecular weight of the binder are, the lower the concentration of the lipid required for achieving a sustained release property. The matrices of HPC EF, VA64 and 12PF utilized 10%, 12.5% and 20% lipid concentrations to sustain drug release, respectively. The optimized drug release profiles of TSMG for all the hydrophilic binders studied, namely, HPC EF (F13), VA64 (F14), and 12PF (F15 & F16), are shown in Fig. 6(D).

The physical blends of the optimized TSMG formulations (F13-F16) were directly compressed (F17-F20) and evaluated for drug release for a comparison with the TSMG profiles. The drug release profiles of the DC matrices were similar to those of the TSMG profiles. The similarity (f2) and dissimilarity (f1) factors were calculated, where f2 and f1 were>75 and<5, indicating good correlation between the profiles of the TSMG and DC matrices. Supplementary Fig. 1 shows the dissolution profiles of the DC formulations (HPC EF – F17; VA64 – F18; 12PF – F19 & F20).

3.9. Drug release kinetics

The correlation coefficient (R^2) and diffusional coefficient (n) estimated using various mathematical models are delineated in Table 3. The release kinetics were interpreted for all the optimized formulations of the TSMG and DC matrices. From the obtained data, it is clear that the incorporation of different binders influenced the release behavior of quetiapine from the matrices rather than the manufacturing process. Irrespective of the manufacturing process matrices of formulations containing HPC EF (F13, F17) followed zero-order release kinetics (R^2 = 0.997) where release of drug from the matrix followed super case II type of diffusion (n > 0.89). The zero-order release of the system can be attributed to a constant surface area with a controlled erosion/swelling of the matrix [46]. Within the matrices of formulations containing VA64 (F14, F18) and 12PF (F15, F16, F19 and F20), the drug release was influenced by change in surface area and diameter of the cylindrical matrix, however the release mechanism of drug was primarily governed by super case II type of diffusion.

3.10. Erosion index

The optimized formulations of the TSMG (F13 - F16) and DC (F17 - F20) matrices were studied for matrix erosion with respect to time in dissolution media. The study was conducted to monitor the behavior of the matrix as a function of time, as it influences the release of drug from sustained release formulations [47]. The erosion profiles of all the studied formulations are captured in Fig. 7. The erosion of the matrix is found to be in line with the dissolution profiles, and the erosion of the matrices follows the order of the binder viscosity. The matrices disintegrated completely before the endpoint of dissolution. The loss of the matrix mass in the first hour (1 h) of the erosion study can be attributed to the dissolution of the drug and binder on the surface. At the end of 1 h, the matrix surface was found to be rough with small perforations. The matrices of 12PF (F15 & F16), one with a faster dissolution rate (F15) and the other with slower dissolution rate (F16), are in line with the erosion results. The matrices of batch F15 eroded faster (10 h) than matrices of F16 (12 h). Thus, erosion studies help to support the dissolution behavior of the matrices.

3.11. Lipid distribution

Dye-coated lipid formulations of TSMG and DC were monitored for the distribution of the lipid after storage for three months at 40 ± 2 °C/75 ± 5% RH. The appearance of the lipid distribution before and after storage is shown in Fig. 8. The surface of matrices prepared by DC revealed a non-uniform distribution of the lipid, and upon storage, enriched layers of the lipids were observed on the surface, which was attributed to their phase separation. However, no such observations were recorded for the matrices prepared by TSMG, preserving its stability. The lipid distribution was found to be uniform before and after storage of the TSMG matrices. Mechanical shear and intense mixing of TSMG distributed the molten materials uniformly between the formulation ingredients. The distribution of the softened binder along the lipid carrier might have resulted in hindered phase separation by preserving the stability of the formulations prepared by TSMG.

Table 3
Release kinetics of twin screw melt granulation (F13-F16) and direct compression formulations (F17-F20).

Model/Batch#	F13	F14	F15	F16	F17	F18	F19	F20
Zero-order (R^2)	0.997	0.896	0.838	0.937	0.995	0.892	0.854	0.951
First-order (R^2)	0.721	0.943	0.877	0.925	0.655	0.951	0.887	0.899
Higuchi (R^2)	0.969	0.98	0.946	0.986	0.975	0.979	0.955	0.986
Korsmeyer-Peppas (R^2)	0.900	0.978	0.988	0.975	0.912	0.981	0.983	0.964
Diffusional coefficient (n)	1.24	1.14	1.345	1.343	1.229	1.119	1.327	1.33
Hixson-crowell (R^2)	0.893	0.995	0.993	0.996	0.884	0.995	0.991	0.992

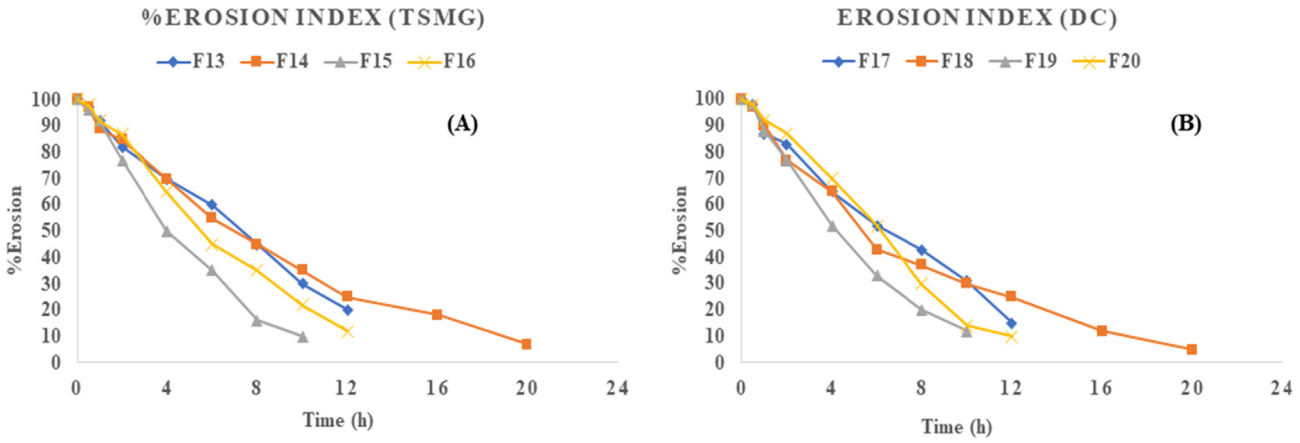

Fig. 7. Erosion studies of the optimized formulations in dissolution media (A) formulations of melt granulation and (B) formulations of direct compression.

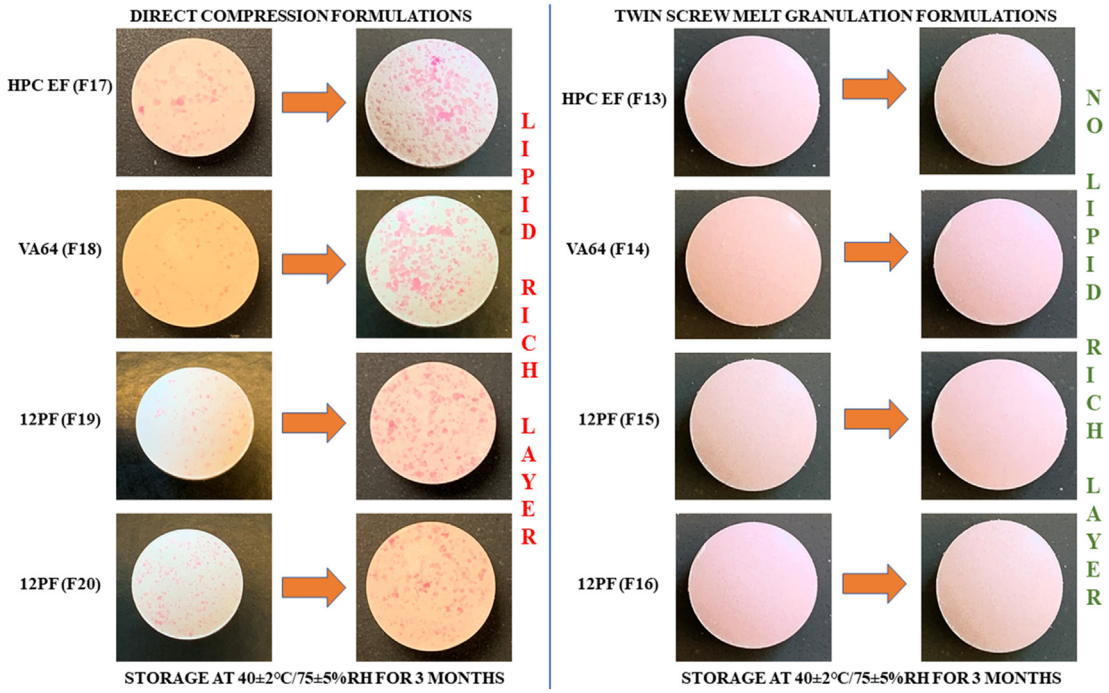

Fig. 8. Distribution of the lipid in matrices prepared by TSMG and DC (before and after storage at 40 ± 2℃/75 ± 5% RH for 3 months).

3.12. Stability studies

The matrices of TSMG (F13-F16) and DC (F17-F20) were evaluated for dissolution, content uniformity, and hardness after storage for 1, 2, 3, and 6 months at 40 ± 2℃/75 ± 5%RH. Thermal scans (DSCs) were also performed on the TSMG samples (F13-F16) to observe the nature of the lipid and drug as a result of storage. All the DSC scans conducted for the stability samples (matrices) after 6 months demonstrated similar melting peaks as initial samples, indicating crystalline nature of QTF and lipid. All the evaluations performed revealed the stability of the TSMG samples over DC. The dissolution profiles of the TSMG samples were in line with those of the initial data, and the calculated f2 (>50) and f1(2–5) factors were found to be acceptable, whereas DC samples resulted in dose dumping with the complete release of the drug in 4 h after storage at accelerated conditions for 1 month. The dose dumping characteristic of the direct compression formulations can be attributed to the loss of matrix integrity and phase separation of the lipid upon storage; these results are in accordance with lipid distribution studies. The hardness of the direct compression matrices dropped to 6.0–8.0 kp, whereas no change in the matrix integrity of the TSMG samples was observed. The hardness of melt granulation formulations was preserved (10–12 kp). The loss of matrix integrity of the DC samples can be attributed to the non-uniform distribution of formulation components due to poor flow and poor compressibility of the blend. Nokhodchi, A et al. [48] evaluated the physical stability of direct compression formulations containing HPMC, and similar observations of reduced matrix integrity upon storage were reported. The stability of the TSMG samples can be attributed to the uniform distribution of formulation ingredients, where all the non-molten materials are entrapped in the granule with the aid of the molten lipid and softened binder, resulting in enhanced flow, compressibility, and uniformity of the formulation. The distribution of the softened binder along the molten lipid might have hindered the movement of the lipid to the surface by generating a stable matrix formulation. The thermal scans carried

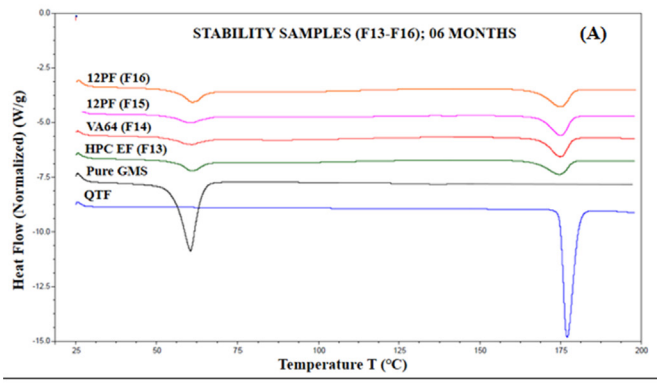

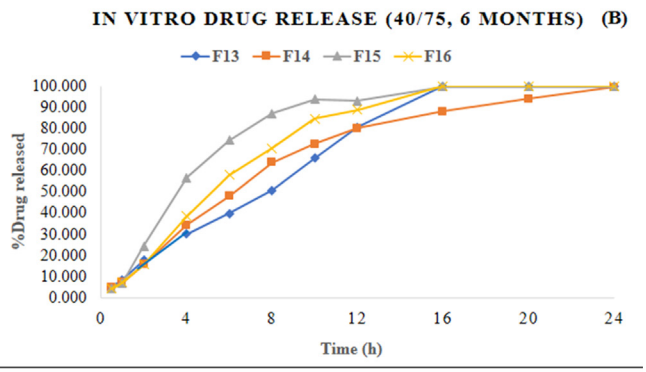

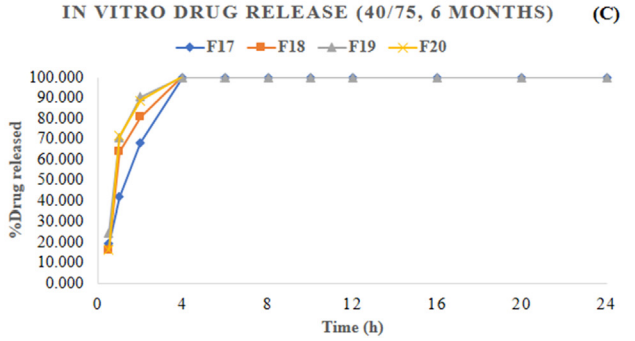

(D)

EVALUATION OF STABILITY SAMPLES (40/75; 6 months)

Batch#	f2	f1	Hardness (KP)	Content Uniformity (%)
F13	79	6	11.32±0.23	100.32±0.23
F14	76	6	11.22±0.11	99.89±0.11
F15	75	5	11.21±0.45	101.01±0.03
F16	74	4	11.31±0.19	99.91±0.11
F17	20	69	7.89±0.29	98.78±0.21
F18	21	65	6.95±0.19	99.65±0.41
F19	20	63	6.21±0.11	100.91±0.37
F20	23	70	6.51±0.33	98.91±0.12

Fig. 9. Stability data of the melt granulation (F13-F16) and direct compression (F17-F20) formulations. (A) DSC scans. (B) In vitro dissolution of the melt granulation formulations; 40/75 condition, 6 months. (C) In vitro dissolution of direct compression; 40/75 condition, 6 months. (D) Results of the matrix hardness, content uniformity, similarity and dissimilarity factors.

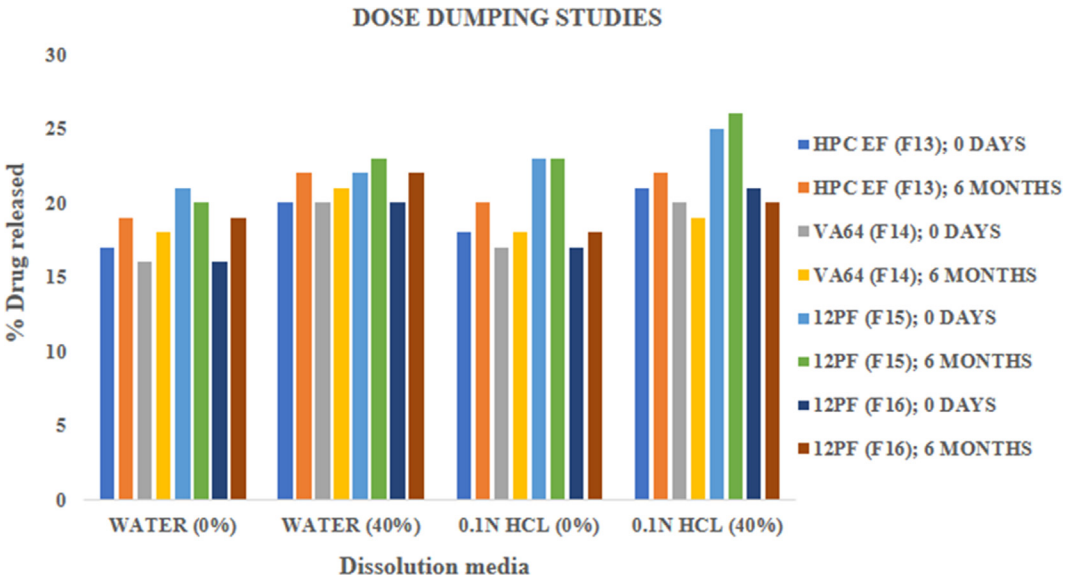

Fig. 10. Dose dumping studies of the TSMG formulations (F13-F16; 0 days and 6 months).

out for the stability samples revealed no shift in the endothermic peak of the lipid, indicating their stability and crystalline nature. The content uniformity of the TSMG and DC matrices was found to be 98.6–101.5%. The evaluated data for the stability samples of TSMG and DC formulations are captured in Fig. 9.

3.13. Dose dumping

Based on the stability results of the TSMG formulations, the formulations (F13-F16) were subjected to AIDD studies in water and 0.1 N HCl with 0% and 40% ethanol. The results of the dose dumping studies are depicted in Fig. 10. All the studied formulations exhibited stable release profiles with no dose dumping behavior in non-alcoholic (0%) and alcoholic media (40%) for 2 h, and the obtained profiles are in line with the in vitro dissolution profiles. The presence of alcohol (40%) influenced the drug release characteristics compared with drug release in dissolution media (water and 0.1 N HCl, (0% ethanol)) without ethanol. However, the f2 values for the dissolution profiles in water and 0.1 N HCl with (40%) and without (0%) alcohol were found to be 90 and 85, respectively,

indicating similar dissolution profiles. The stability of the matrix can be attributed to the insoluble nature and poor wetting property of the lipid carrier. The mechanical shear and intense mixing of materials distributed the molten lipid carrier uniformly through the formulation blend, thus protecting the stability of the matrix from the external environment. The maximum amount of drug release was found to be 26% (F15) in 0.1 N HCl consisting of 40% alcohol. Thus, TSMG provides an added advantage for developing dosage forms that can resist dose dumping characteristics.

4. Conclusion

TSMG was successfully performed for all the studied formulations by incorporating softened hydrophilic binders into a molten lipid carrier. A low binder concentration (5%) resulted in successful granule formation, where the granule size and number were influenced by increasing the lipid concentration, viscosity, and molecular weight of the binders. The granules and compressed matrices of TSMG exhibited improved flow and tableting properties over the formulations manufactured by the DC technique. The drug load, lipid, and diluent concentrations played crucial roles in optimizing the drug release profiles. All the formulations of TSMG and DC resulted in the sustained release of the drug for 16–24 h. Upon storage under accelerated conditions (40 ± 2℃/75 ± 5% RH) for 6 months, the sustained release property of the TSMG formulations was preserved, whereas the DC formulations resulted in drug dose dumping attributed to the loss of matrix integrity and the phase separation of the lipid carrier. The matrices of TSMG were resistant to dose dumping studies at a 40% alcohol level. The mechanical shear and intense mixing property of TSMG resulted in a uniform distribution of the molten lipid carrier and hydrophilic binders by promoting the stability of the SR formulations. This study reveals TSMG as an advanced alternative continuous granulation technique for developing stable lipid-based matrix formulations. However, the above results suggest that incorporation of hydrophilic binders into the molten lipid carrier by TSMG may be applicable to develop stable SR formulations.

Funding

This project was also partially supported by Grant Number P30GM122733-01A1, funded by the National Institute of General Medical Sciences (NIGMS), a component of the National Institutes of Health (NIH) as one of its Centers of Biomedical Research Excellence (COBRE).

Declaration of Competing Interest

The authors declare that they have no known competing financial interests or personal relationships that could have appeared to influence the work reported in this paper.

Acknowledgements

The authors thank Ashland, Gattefosse and BASF for providing the polymers. The scanning electron microscopy images presented in this work were generated using the instruments and services at the Microscopy and Imaging Center, The University of Mississippi. This facility is supported in part by grant 1726880, the National Science Foundation.

Appendix A. Supplementary material

Supplementary data to this article can be found online at https://doi.org/10.1016/j.apt.2021.05.040.

References

[1] P. Viswanathan, Y. Muralidaran, G. Ragavan, Challenges in oral drug delivery: A nano-based strategy to overcome, in: Nanostructures Oral Med., (2017) pp. 173–201. https://doi.org/10.1016/B978-0-323-47720-8.00008-0.
[2] R.J. Dias, S.S. Sakhare, K.K. Mali, Design and development of mucoadhesive acyclovir tablet, Iran. J. Pharm. Res. 8 (2009) 231–239, https://doi.org/10.22037/ijpr.2010.816.
[3] CDER, New Drugs at FDA: CDER's New Molecular Entities and New Therapeutic Biological Products, FDA. (2016). https://www.fda.gov/drugs/development-approval-process-drugs/new-drugs-fda-cders-new-molecular-entities-and-new-therapeutic-biological-products (accessed October 23, 2020).
[4] J.W. Wheless, S.J. Phelps, A clinician's guide to oral extended-release drug delivery systems in epilepsy, J. Pediatr. Pharmacol. Ther. 23 (2018) 277–292, https://doi.org/10.5863/1551-6776-23.4.277.
[5] M. Trofimiuk, K. Wasilewska, K. Winnicka, How to modify drug release in paediatric dosage forms? Novel technologies and modern approaches with regard to children's population, Int. J. Mol. Sci. 20 (2019) 3200, https://doi.org/10.3390/ijms20133200.
[6] L. Meeus, Direct compression versus granulation, Pharm. Technol. Eur. 23 (2011) 21–22 (accessed October 23, 2020) https://www.pharmtech.com/view/direct-compression-versus-granulation.
[7] A.Q. Vo, J. Zhang, D. Nyavanandi, S. Bandari, M.A. Repka, Hot melt extrusion paired fused deposition modeling 3D printing to develop hydroxypropyl cellulose based floating tablets of cinnarizine, Carbohydr. Polym. 246 (2020), https://doi.org/10.1016/j.carbpol.2020.116519 116519.
[8] S. Bandari, D. Nyavanandi, V.R. Kallakunta, K.Y. Janga, S. Sarabu, A. Butreddy, M. A. Repka, Continuous twin screw granulation – an advanced alternative granulation technology for use in the pharmaceutical industry, Int. J. Pharm. 580 (2020), https://doi.org/10.1016/j.ijpharm.2020.119215 119215.
[9] A. Butreddy, D. Nyavanandi, S. Narala, F. Austin, S. Bandari, Application of hot melt extrusion technology in the development of abuse deterrent formulations: an overview, Curr. Drug Deliv. 17 (2020), https://doi.org/10.2174/1567201817999200817151601.
[10] S. Narala, D. Nyavanandi, P. Srinivasan, P. Mandati, S. Bandari, M.A. Repka, Pharmaceutical Co-crystals, Salts, and Co-amorphous Systems: A novel opportunity of hot-melt extrusion, J. Drug Deliv. Sci. Technol. In press (2020) 102209. https://doi.org/10.1016/j.jddst.2020.102209.
[11] S. Bandari, D. Nyavanandi, N. Dumpa, M.A. Repka, Coupling Hot Melt Extrusion and Fused Deposition Modeling: Critical Properties for Successful Performance, Elsevier. In Press (2021). https://doi.org/10.1016/j.addr.2021.02.006.
[12] J. Hamdani, A.J. Moës, K. Amighi, Development and evaluation of prolonged release pellets obtained by the melt pelletization process, Int. J. Pharm. 245 (2002) 167–177, https://doi.org/10.1016/S0378-5173(02)00348-4.
[13] C. Reitz, P. Kleinebudde, Influence of thermal and thermo-mechanical treatment : Comparison of two lipids with respect to their suitability for solid lipid extrusion, J. Therm. Anal. Calorim. 89 (2007) 669–673, https://doi.org/10.1007/s10973-006-7953-z.
[14] C. Reitz, P. Kleinebudde, Solid lipid extrusion of sustained release dosage forms, Eur. J. Pharm. Biopharm. 67 (2007) 440–448, https://doi.org/10.1016/j.ejpb.2007.03.008.
[15] M.H. Aburahma, S.M. Badr-Eldin, Compritol 888 ATO: A multifunctional lipid excipient in drug delivery systems and nanopharmaceuticals, Expert Opin. Drug Deliv. 11 (2014) 1865–1883, https://doi.org/10.1517/17425247.2014.935335.
[16] GeleolTM Mono and Diglycerides NF - Glycerol monostearate - Oily vehicle. https://www.gattefosse.com/pharmaceuticals-products/geleol-mono-and-diglycerides-nf (accessed March 10, 2021).
[17] H. Patil, R.V. Tiwari, S.B. Upadhye, R.S. Vladyka, M.A. Repka, Formulation and development of pH-independent/dependent sustained release matrix tablets of ondansetron HCl by a continuous twin-screw melt granulation process, Int. J. Pharm. 496 (2015) 33–41, https://doi.org/10.1016/j.ijpharm.2015.04.009.
[18] T. Higuchi, Mechanism of sustained-action medication. theoretical analysis of rate of release of solid drugs dispersed in solid matrices, J. Pharm. Sci. 52 (1963) 1145–1149, https://doi.org/10.1002/jps.2600521210.
[19] A.W. Hixson, J.H. Crowell, Dependence of Reaction Velocity upon surface and Agitation: I-Theoretical Consideration, Ind. Eng. Chem. 23 (1931) 923–931, https://doi.org/10.1021/ie50260a018.
[20] R.W. Korsmeyer, R. Gurny, E. Doelker, P. Buri, N.A. Peppas, Mechanisms of solute release from porous hydrophilic polymers, Int. J. Pharm. 15 (1983) 25–35, https://doi.org/10.1016/0378-5173(83)90064-9.
[21] P. Costa, J.M. Sousa Lobo, Modeling and comparison of dissolution profiles, Eur. J. Pharm. Sci. 13 (2001) 123–133, https://doi.org/10.1016/S0928-0987(01)00095-1.
[22] H. Baishya, Application of mathematical models in drug release kinetics of carbidopa and levodopa ER tablets, J. Dev. Drugs. 06 (2017) 1–8, https://doi.org/10.4172/2329-6631.1000171.
[23] L. Wang, K. Chen, H. Wen, D. Ouyang, X. Li, Y. Gao, W. Pan, X. Yang, Design and Evaluation of Hydrophilic Matrix System Containing Polyethylene Oxides for the Zero-Order Controlled Delivery of Water-Insoluble Drugs, AAPS PharmSciTech. 18 (2017) 82–92, https://doi.org/10.1208/s12249-016-0498-y.
[24] V. Pillay, R. Fassihi, Evaluation and comparison of dissolution data derived from different modified release dosage forms: An alternative method, J.

Control. Release. 55 (1998) 45–55, https://doi.org/10.1016/S0168-3659(98)00022-4.
[25] L. Kassaye, G. Genete, Evaluation and comparison of in-vitro dissolution profiles for different brands of amoxicillin capsules, Afr. Health Sci. 13 (2013) 369–375, https://doi.org/10.4314/ahs.v13i2.25.
[26] S. D'Souza, S. Mayock, A. Salt, A review of in vivo and in vitro aspects of alcohol-induced dose dumping, AAPS Open. 3 (2017) 1–20, https://doi.org/10.1186/s41120-017-0014-9.
[27] B. Van Melkebeke, B. Vermeulen, C. Vervaet, J.P. Remon, Melt granulation using a twin-screw extruder: A case study, Int. J. Pharm. 326 (2006) 89–93, https://doi.org/10.1016/j.ijpharm.2006.07.005.
[28] M. Vasanthavada, Y. Wang, T. Haefele, J.P. Lakshman, M. Mone, W. Tong, Y.M. Joshi, A.T. Abu, Application of melt granulation technology using twin-screw extruder in development of high-dose modified-release tablet formulation, J. Pharm. Sci. 100 (2011) 1923–1934, https://doi.org/10.1002/jps.22411.
[29] J. Li, L. Tao, D. Buckley, J. Tao, J. Gao, M. Hubert, Effect of physical states of binders on high-shear wet granulation and granule properties: A mechanistic approach toward understanding high-shear wet granulation process, part 3: Effect of binder rheological properties, J. Pharm. Sci. 101 (2012) 1877–1887, https://doi.org/10.1002/jps.23059.
[30] Y. Liu, M.R. Thompson, K.P. O'Donnell, Impact of non-binder ingredients and molecular weight of polymer binders on heat assisted twin screw dry granulation, Int. J. Pharm. 536 (2018) 336–344, https://doi.org/10.1016/j.ijpharm.2017.11.061.
[31] Ashland, Klucel hydroxy-propyl-cellulose. https://www.ashland.com/file_source/Ashland/Product/Documents/Pharmaceutical/PC_11229_Klucel_HPC.pdf (accessed March 9, 2021).
[32] K. Kolter, M. Karl, A. Gryczke, Hot melt extrusion with BASF pharma polymers, 2012. https://www.google.com/search?q=hot+melt+extrusion+with+BASF+pharma+polymers&rlz=1C1CHBD_enUS743US743&oq=hot+melt+extrusion+with+BASF+pharma+polymers&aqs=chrome..69i57j0i22i30l2.12476j0j9&sourceid=chrome&ie=UTF-8 (accessed March 9, 2021).
[33] T. De Pilli, B.F. Carbone, A.G. Fiore, C. Severini, Effect of some emulsifiers on the structure of extrudates with high content of fat, J. Food Eng. 79 (2007) 1351–1358, https://doi.org/10.1016/j.jfoodeng.2006.04.054.
[34] R.M. Dhenge, K. Washino, J.J. Cartwright, M.J. Hounslow, A.D. Salman, Twin screw granulation using conveying screws: effects of viscosity of granulation liquids and flow of powders, Powder Technol. 238 (2013) 77–90, https://doi.org/10.1016/j.powtec.2012.05.045.
[35] E.Z. Dahmash, A.R. Mohammed, Functionalised particles using dry powder coating in pharmaceutical drug delivery: promises and challenges, Expert Opin. Drug Deliv. 12 (2015) 1867–1879, https://doi.org/10.1517/17425247.2015.1071351.
[36] T.M. Chitu, D. Oulahna, M. Hemati, Wet granulation in laboratory scale high shear mixers: effect of binder properties, Powder Technol. 206 (2011) 25–33, https://doi.org/10.1016/j.powtec.2010.07.012.
[37] P.J.T. Mills, J.P.K. Seville, P.C. Knight, M.J. Adams, The effect of binder viscosity on particle agglomeration in a low shear mixer/agglomerator, Powder Technol. 113 (2000) 140–147, https://doi.org/10.1016/S0032-5910(00)00224-2.
[38] J.M. Keen, C.J. Foley, J.R. Hughey, R.C. Bennett, V. Jannin, Y. Rosiaux, D. Marchaud, J.W. McGinity, Continuous twin screw melt granulation of glyceryl behenate: Development of controlled release tramadol hydrochloride tablets for improved safety, Int. J. Pharm. 487 (2015) 72–80, https://doi.org/10.1016/j.ijpharm.2015.03.058.
[39] J. Hamdani, A.J. Moës, K. Amighi, Physical and thermal characterisation of Precirol® and Compritol® as lipophilic glycerides used for the preparation of controlled-release matrix pellets, Int. J. Pharm. 260 (2003) 47–57, https://doi.org/10.1016/S0378-5173(03)00229-1.
[40] M. Akhlaq, F. Maryam, A. Elaissari, H. Ullah, M. Adeel, A. Hussain, M. Ramzan, O. Ullah, M.Z. Danish, S. Iftikhar, N. Aziz, Pharmacokinetic evaluation of quetiapine fumarate controlled release hybrid hydrogel: A healthier treatment of schizophrenia, Drug Deliv. 25 (2018) 916–927, https://doi.org/10.1080/10717544.2018.1458922.
[41] E. Pretsch, P. Bühlmann, M. Badertscher, Structure determination of organic compounds: Tables of spectral data, 2009th ed., Springer, 2009. https://doi.org/10.1007/978-3-540-93810-1.
[42] T. Hussain, T. Saeed, A.M. Mumtaz, Z. Javaid, K. Abbas, A. Awais, H.A. Idrees, Effect of two hydrophobic polymers on the release of gliclazide from their matrix tablets, Acta Pol. Pharm. - Drug Res. 70 (2013) 749–757. https://pdfs.semanticscholar.org/2640/4f61f314e925ab5d94bfecb30743a7f5a7a8.pdf. (accessed October 23, 2020).
[43] A. Gardouh, Design and Characterization of Glyceryl Monostearate Solid Lipid Nanoparticles Prepared by High Shear Homogenization, Br. J. Pharm. Res. 3 (2013) 326–346, https://doi.org/10.9734/bjpr/2014/2770.
[44] K.R. Chu, E. Lee, S.H. Jeong, E.S. Park, Effect of particle size on the dissolution behaviors of poorly water-soluble drugs, Arch. Pharm. Res. 35 (2012) 1187–1195, https://doi.org/10.1007/s12272-012-0709-3.
[45] K. Vithani, M. Maniruzzaman, I.J. Slipper, S. Mostafa, C. Miolane, Y. Cuppok, D. Marchaud, D. Douroumis, Sustained release solid lipid matrices processed by hot-melt extrusion (HME), Colloids Surfaces B Biointerfaces. 110 (2013) 403–410, https://doi.org/10.1016/j.colsurfb.2013.03.060.
[46] Q. Liu, R. Fassihi, Zero-order delivery of a highly soluble, low dose drug alfuzosin hydrochloride via gastro-retentive system, Int. J. Pharm. 348 (2008) 27–34, https://doi.org/10.1016/j.ijpharm.2007.07.009.
[47] X. Yin, H. Li, Z. Guo, L. Wu, F. Chen, M. De Matas, Q. Shao, T. Xiao, P. York, Y. He, J. Zhang, Quantification of swelling and erosion in the controlled release of a poorly water-soluble drug using synchrotron x-ray computed microtomography, AAPS J. 15 (2013) 1025–1034, https://doi.org/10.1208/s12248-013-9498-y.
[48] A. Nokhodchi, Y. Javadzadeh, The effect of storage conditions on the physical stability of tablets, Pharm. Technol. Eur. 19 (2007) 20–26 (accessed October 23, 2020) https://www.researchgate.net/publication/285964163.